Available online at www.sciencedirect.com
ScienceDirect
Journal of Catalysis 243 (2006) 428–437
JOURNAL OF CATALYSIS
www.elsevier.com/locate/jcat

Rate and oxygen activity oscillations during propane oxidation on Pt/YSZ

Christos Kokkofitis, Michael Stoukides *

Chemical Engineering Department and Chemical Process Engineering Research Institute, University Box 1517, University Campus, Thessaloniki 54124, Greece

Received 9 May 2006; revised 3 July 2006; accepted 29 July 2006

Abstract

The catalytic oxidation of propane on polycrystalline platinum films supported on yttria-stabilized zirconia was studied at 573–773 K and atmospheric total pressure. The technique of solid electrolyte potentiometry (SEP) was used to monitor the thermodynamic activity of oxygen adsorbed on the catalyst surface during reaction. Over a wide range of temperature and gas-phase composition, both the reaction rate and the surface oxygen activity were found to exhibit self-sustained isothermal oscillatory behavior. Reaction rate and oxygen activity oscillated simultaneously. Sustained oscillations were observed when the reactant ratio, $P_{O_2}/P_{C_3H_8}$, was kept between 1.2 and 2.2. At temperatures above 723 K, only stable steady states were obtained. The reaction kinetics and primarily the SEP data strongly indicate that the oscillatory phenomena are related to periodic formation and decomposition of a surface platinum oxide.

Keywords: Propane oxidation on Pt; Solid electrolyte potentiometry; Rate and oxygen activity oscillations

1. Introduction

Interest in the catalytic oxidation of hydrocarbons has increased over the last two decades, because it provides an environmentally acceptable alternative to conventional flame combustion. Compared with alkenes, stable lower alkanes require higher temperatures for complete oxidation, and platinum is considered the most active catalyst for the combustion of propane [1–5]. In an effort to further enhance the catalytic activity of Pt, numerous investigators have studied this reaction focusing on (a) the role of the support [3–7], (b) the effect of particle size and catalyst dispersion [1,2,8], and (c) the effects of solid additives and gas-phase promoters [3,9–12]. Recently, as an alternative approach to catalytic promotion, the effect of electrochemical promotion (NEMCA) also has been investigated by studying the reaction in solid electrolyte cells [13–15].

In one of these studies [15], it was found that under certain conditions the reaction rate exhibits oscillatory behavior. The phenomenon of sustained oscillations in catalytic reactions is not new; it was first reported in the late 1960s [16–18]. Since then, numerous reaction systems have been reported to exhibit such phenomena, and several comprehensive reviews on this interesting subject have been published. The earlier studies were reviewed by Sheintuch and Schmitz [19] and Slin'ko and Slin'ko [20]. Works before 1985 were reviewed by Razon and Schmitz [21], and more recent works were reviewed by Shuth et al. [22], Slin'ko and Jaeger [23], and Imbihl and Ertl [24].

The oxidation of propane was not listed as an oscillatory reaction in any of these reviews. In 2001, Gladky et al. [25] reported oscillations during the catalytic oxidation of propane over a nickel wire. Oscillations were observed between 923 and 1023 K and at very low oxygen/propane ratios. The periodic changes in the reactant concentrations were accompanied by significant synchronous fluctuations of the catalyst temperature. The same research group further investigated these phenomena using in situ thermography and X-ray photoelectron spectroscopy [26,27].

Sustained oscillations in the catalytic oxidation of propane on Pt were first reported in our previous work, in which the effect of electrochemical promotion was studied in a solid electrolyte cell [15]. The present communication is a detailed study of the observed oscillations. Using the same experimental apparatus, the dependence of the characteristics of the oscillations (period, shape, etc.) on reactant composition, temperature, and volumetric flow rate is determined. Moreover, the oxy-

* Corresponding author. Fax: +30 2310 996145.
E-mail address: stoukidi@cperi.certh.gr (M. Stoukides).

0021-9517/$ – see front matter
doi:10.1016/j.jcat.2006.07.032

gen/propane ratio and the temperature region within which the reaction exhibits oscillatory behavior are established. In addition to reaction rate measurements, the technique of solid electrolyte potentiometry (SEP) is used to monitor the thermodynamic activity of oxygen adsorbed on the catalyst surface. The SEP data are combined with reaction kinetics in an effort to interpret these interesting unsteady-state phenomena.

2. Experimental

The experimental apparatus as well as the solid electrolyte cell-reactor used in this study, have been described in detail in a previous communication [15]. The cell-reactor consisted of an 8 mol% yttria-stabilized zirconia (YSZ) tube (15 cm long, 16 mm i.d., 19 mm o.d.) closed at its bottom end. Under the conditions of the present experiments, this material is a pure oxygen ion (O^{2-}) conductor. Reactant gases, C_3H_8, O_2, and diluent He were of 99.999% purity. The analysis of the inlet (C_3H_8, O_2) and outlet gases (C_3H_8, O_2, CO_2, H_2O) was performed using an on-line, gas chromatograph (Shimadzu GC-14B) with a thermal conductivity detector (TCD). A Porapak QS column was used to separate C_3H_8, CO_2, and H_2O, and a 13X molecular sieve was used to separate O_2. The concentrations of CO and CO_2 were also continuously monitored using a Binos infrared CO and CO_2 analyzer. The reactor was located in a furnace, the temperature of which was controlled within ± 2 K from the set point.

The polycrystalline porous Pt catalyst electrode, prepared from a Pt paste (Engelhard A1121), was deposited at the inside bottom of the YSZ tube. Then it was calcined in air for 60 min at 1023 K. The catalyst loading was 260 mg. Scanning electron microscopy examination of the catalyst showed an average particle size of the crystallites of about 0.4 μm. Using the catalyst loading and the average particle size of the Pt crystallites, a catalytic surface area of approximately 1850 cm^2 was calculated.

Similarly, a Ag reference electrode was deposited on the outer side of the tube and was exposed to ambient air. The Ag reference electrode was prepared from a Ag paste (GC Electronics No. 22-202). Silver was used as the auxiliary electrode material because it adheres very strongly to the zirconia outside surface. The electrode was calcined in air for 1 h at 923 K. The superficial surface area of both the working and reference electrodes was 5 cm^2.

In the present experiments, the cell reactor operated under open circuit only, that is, with no current passing through the solid electrolyte. This operation does not differ from that of a regular catalytic reactor; both reactants are co-fed as gaseous C_3H_8 and O_2. Nevertheless, the catalytic reaction rate measurements can be combined with open-circuit voltage data using SEP. The principle of SEP is simple: One of the electrodes is exposed to the reacting mixture and thus serves as a catalyst for the reaction under study, and the other electrode is exposed to the air and serves as a reference electrode. It has been shown [28–33] that the thermodynamic activity of atomically adsorbed oxygen, α_o, is given by the equation

$$\alpha_o = (0.21)^{1/2} \exp(2FE/RT), \quad (1)$$

where F is the Faraday constant, R is the ideal gas constant, T is the absolute temperature, and E is the electromotive force (emf) of the cell. The validity of Eq. (1) is based on several assumptions [30,32], among which the most important is that atomically adsorbed oxygen is the only species to equilibrate rapidly with oxygen ions at the three-phase (gas–electrode–electrolyte) interline. SEP has two advantages: it is an in situ technique, and the measurement is continuous. The latter is very helpful in examining transient or oscillatory phenomena on catalytic surfaces. Earlier SEP studies were conducted on metal electrodes, but the technique was later extended to oxide electrodes [32].

3. Results

The reaction temperature varied between 573 and 773 K, whereas the total pressure was 1 atm. The inlet propane partial pressure varied from 0.2 to 2.5 kPa, and that of oxygen varied from 0.15 to 10 kPa. Helium was used as a diluent, and the total volumetric flow rate varied between 40 and 320 cm^3/min. For the above range of volumetric flow rates, the reactor behavior was very close to that of an ideal CSTR [15]. At all temperatures and reactant compositions examined, the only reaction products detected were CO_2 and H_2O. Hence, in all results reported below, the reaction rate ($r_{C_3H_8}$) is expressed in moles of propane consumed per second.

The extent of noncatalytic oxidation of propane has already been evaluated and found to be <3% of the total reaction rate at the highest temperature examined [15]. The kinetic results shown here have been corrected by subtracting the noncatalytic contribution.

3.1. Steady-state kinetics

Fig. 1 shows the dependence of the reaction rate and the surface oxygen activity on the partial pressure of propane, $P_{C_3H_8}$. The partial pressure of oxygen, P_{O_2}, was kept at 3 kPa and the temperature varied from 573 to 773 K. Fig. 1a shows that at all $P_{C_3H_8}$, the reaction rate was positive order in propane. At higher $P_{C_3H_8}$, however, a sharper increase in the reaction rate with $P_{C_3H_8}$ is seen. This change in the slope of rate versus $P_{C_3H_8}$ is not seen at 573 and 623 K. The corresponding α_o data are shown in Fig. 1b. The horizontal dotted line above the α_o data corresponds to the gas-phase $P_{O_2}^{1/2}$ values in the reactor, with $P_{O_2}^{1/2}$ given in $bar^{1/2}$. If thermodynamic equilibrium were established between adsorbed and gaseous oxygen, then the α_o data should fall on the dotted line. The values of α_o vary from 10^{-1} to 10^{-5} and decrease with increasing propane. It can be seen that, in general, high reaction rates correspond to very low α_o values. In addition, at temperatures at which there is no change in the slope of the reaction rate curve (e.g., 573 and 623 K), there is no sharp change in the α_o curve either.

Figs. 2a and 2b show the dependence of reaction rate and surface oxygen activity, respectively, on P_{O_2}. The partial pressure of propane was kept at 1 kPa. At low P_{O_2}, the reaction rate increased drastically until a maximum value is attained, then

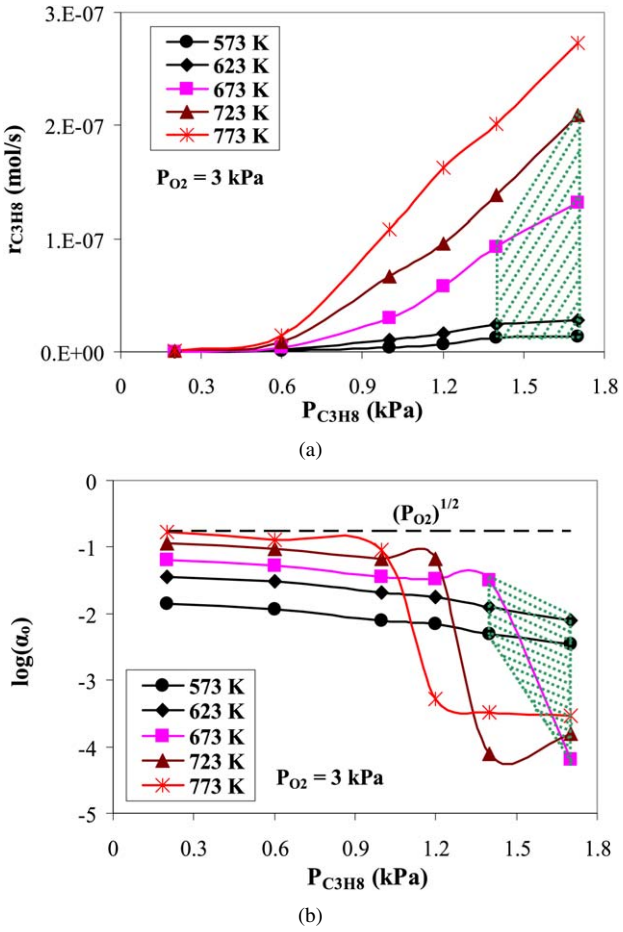

Fig. 1. Dependence of (a) the reaction rate, $r_{C_3H_8}$ and (b) the surface oxygen activity, α_o, on $P_{C_3H_8}$. $P_{O_2} = 3$ kPa.

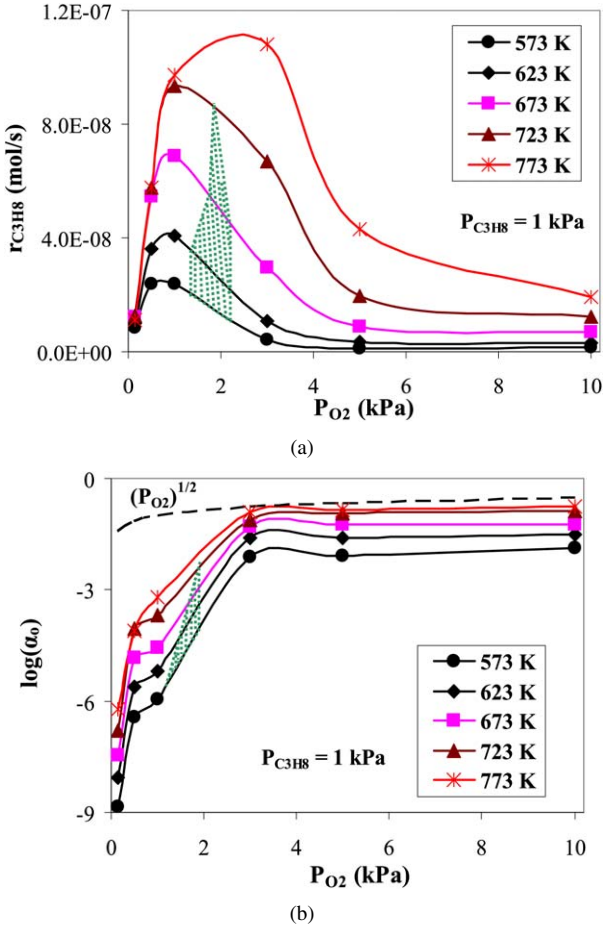

Fig. 2. Dependence of (a) the reaction rate, $r_{C_3H_8}$ and (b) the surface oxygen activity, α_o, on P_{O_2}. $P_{C_3H_8} = 1$ kPa.

decreased sharply; at even higher P_{O_2}, it leveled off to low values. Fig. 2b shows that at P_{O_2} where the reaction rate maxima were observed, the surface oxygen activity was very low.

Excluding those of 573 K, the data of Figs. 1 and 2 have already been reported in a previous communication [15]. They are shown here again because the steady-state kinetics and primarily the oxygen activity behavior (Figs. 1b and 2b) will be used to support the interpretation presented in the Discussion section. Furthermore, in each of these figures there is a shaded area that represents the region of temperature and reactant composition within which the rate and oxygen activity oscillations were observed. It can be seen that oscillations appear when the $P_{O_2}/P_{C_3H_8}$ ratio is between 1.2 and 2.2. Also, Figs. 1b and 2b show that the reaction exhibits oscillations at intermediate α_o values, that is, when $10^{-5} < \alpha_o < 10^{-2}$. These observations are discussed in more detail below.

3.2. Oscillatory states

Oscillatory phenomena were observed at all temperatures except 773 K, the highest temperature studied. The reaction rate oscillations were always accompanied by oxygen activity oscillations. Examples of the reaction rate and the surface oxygen activity behavior versus time are shown in Figs. 3–6. It can be seen that both $r_{C_3H_8}$ and α_o exhibit multipeaked oscillations. The reaction rate and the surface oxygen activity oscillate simultaneously, with increasing $r_{C_3H_8}$ generally corresponding to decreasing α_o. This seems to be in disagreement with some of the data presented in the previous figures. This apparent disagreement occurs because the oxygen activity measurement is instantaneous, whereas the reaction rate is calculated from the exit P_{CO_2} value, which is measured by the CO_2 analyzer. Therefore, there is a delay in the $r_{C_3H_8}$ measurement, which, depending on the effluent volumetric flow rate, may be between 10 and 80 s.

Figs. 3a and 3b show the effect of temperature on $r_{C_3H_8}$ and α_o, respectively, with the inlet gas composition and the total volumetric flow rate kept constant ($P_{C_3H_8} = 1.7$ kPa, $P_{O_2} = 3$ kPa, and $F_t = 84$ ml/min). The temperature varied from 573 to 773 K. It can be clearly seen that the period of the oscillations decreased with increasing temperature. At 573 K, the period was about 10 min, and at 723 K, it was reduced to 40 s. The amplitude of the oscillations, however, seemed to be unaffected by temperature. At 773 K, the oscillatory phenomena disappeared, and a steady-state rate of 2.73×10^{-7} mol/s was obtained.

The effect of the reactant gas composition on $r_{C_3H_8}$ and α_o is shown in Figs. 4 and 5. Figs. 4a and 4b show the effect of $P_{C_3H_8}$ for $T = 673$ K, $P_{O_2} = 3$ kPa, and $F_t = 84$ cm^3/min.

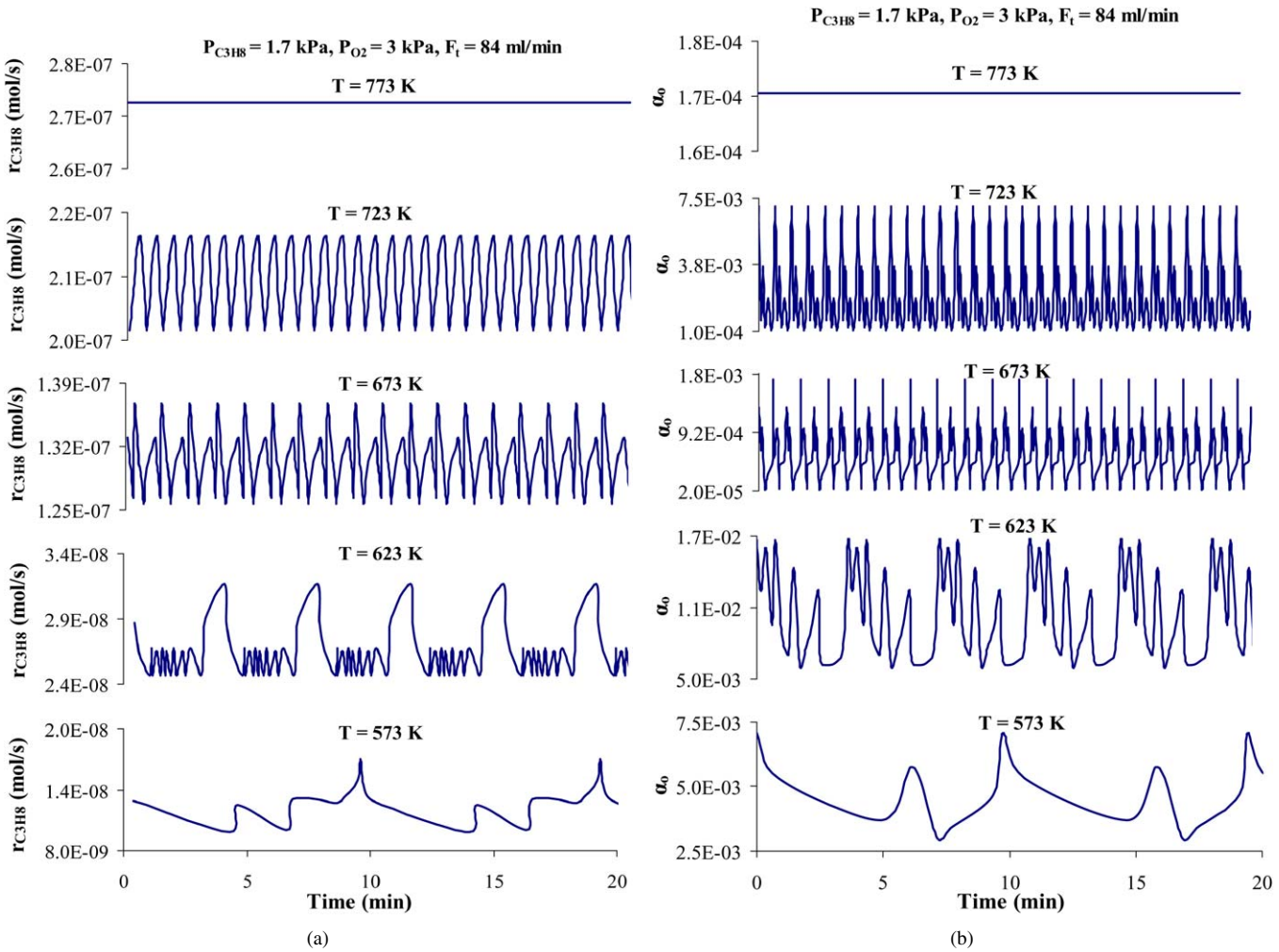

Fig. 3. Temperature effect on (a) $r_{C_3H_8}$ and (b) α_o, at constant gas composition. $P_{C_3H_8} = 1.7$ kPa, $P_{O_2} = 3$ kPa.

At $P_{C_3H_8} = 1.2$ kPa, a steady-state rate of 5.8×10^{-8} mol/s was obtained. At $P_{C_3H_8} = 1.4$ and 1.7 kPa, sustained oscillatory behavior was observed. The period and amplitude of the oscillations increased with increasing $P_{C_3H_8}$. At $P_{C_3H_8} = 2.5$ kPa, the oscillatory phenomena disappeared and a steady-state rate of 1.99×10^{-7} mol/s was obtained. In a similar manner, Figs. 5a and 5b show the effect of P_{O_2} on $r_{C_3H_8}$ and α_o, respectively, for $T = 623$ K, $P_{C_3H_8} = 1.4$ kPa, and $F_t = 84$ cm^3/min. Again, the oscillatory region was bound by two stable steady-state regions. In this particular experiment, oscillations appeared on reaching a minimum of $P_{O_2} = 1.7$ kPa and disappeared when P_{O_2} exceeded 4 kPa.

Figs. 6a and 6b show the effect of volumetric flow rate or, equivalently, residence time in the reactor. The temperature was kept at 623 K, and the inlet composition was kept at $P_{C_3H_8} = 1.4$ kPa and $P_{O_2} = 3$ kPa. The volumetric flow rate, F_t, varied from 40 to 320 cm^3/min. It can be seen that the residence time had an effect only on the period of the oscillations. The period decreased from 200 to 35 s when F_t increased from 40 cm^3/min to 320 cm^3/min. There were no lower and upper limits of F_t within which the reaction exhibited oscillations and there was no effect on the amplitude of the $r_{C_3H_8}$ and α_o fluctuations.

As already mentioned, at each temperature there were lower and upper values of $P_{O_2}/P_{C_3H_8}$ and α_o within which oscillations occur, as depicted in Fig. 7. Fig. 7a shows the $P_{O_2}/P_{C_3H_8}$-temperature region in which the reaction oscillated; the shaded area is the oscillatory region. For $P_{O_2}/P_{C_3H_8} > 2.2$ and $P_{O_2}/P_{C_3H_8} < 1.2$, only stable steady states occurred, and no oscillations occurred above 723 K. Similarly, Fig. 7b shows the α_o region at which the surface oxygen activity exhibited oscillatory behavior. Again, no α_o oscillations occurred above 723 K.

4. Discussion

Many catalytic reactions have been reported to exhibit sustained oscillations, and many models that predict and interpret these oscillations qualitatively or semiquantitatively have been proposed over the last 30 years [19–24]. It has become clear that there is no unique mechanism capable of explaining the oscillatory phenomena in all catalytic reactions. If one focuses on a single catalytic reaction, then the experimental findings may depend on the catalyst used. On a single catalyst, many catalytic systems may oscillate, each having different experimental characteristics. For example, reactions that oscillate on Pt catalysts

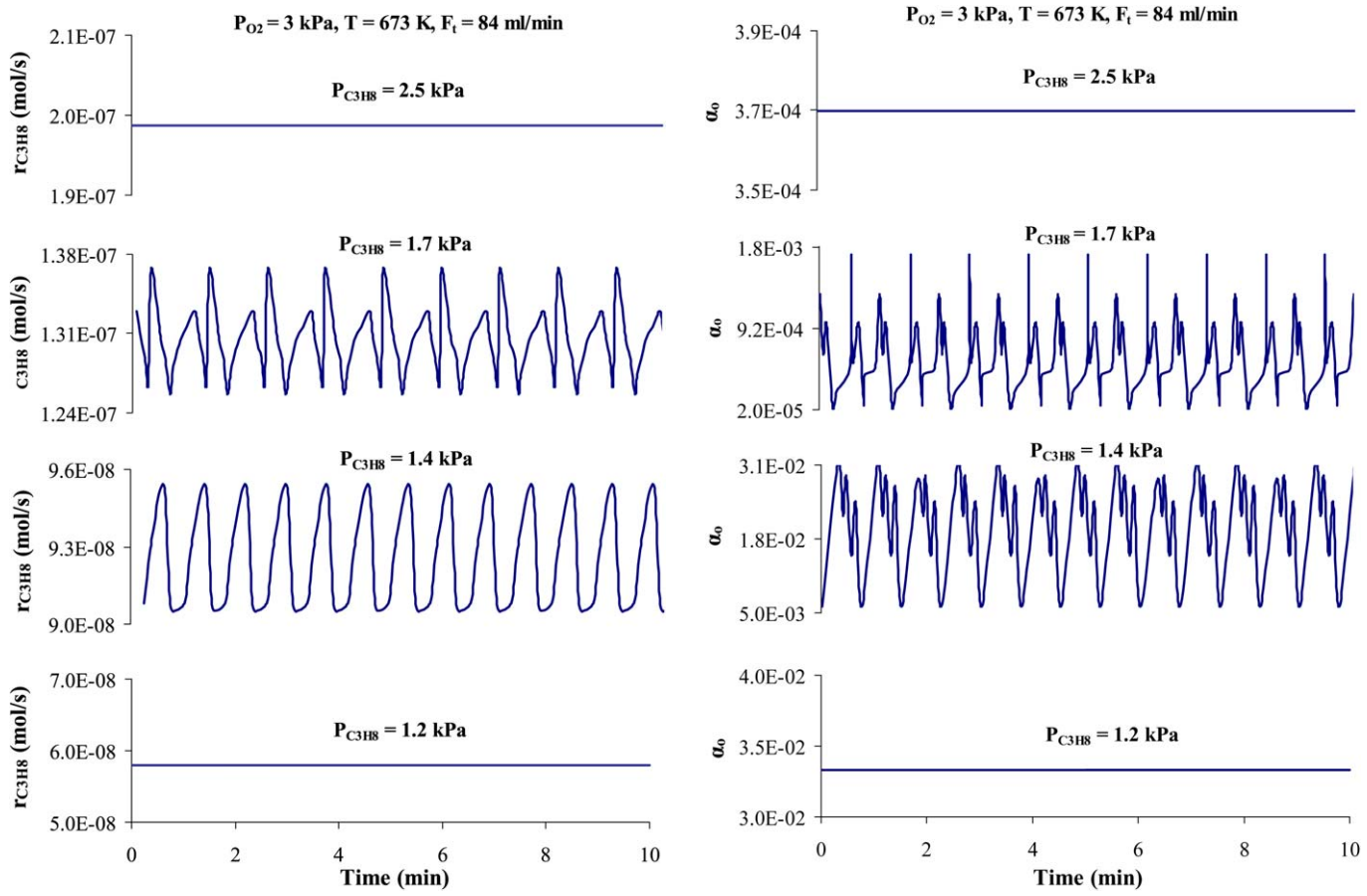

Fig. 4. Effect of $P_{C_3H_8}$ on (a) $r_{C_3H_8}$ and (b) α_o, at constant temperature. $T = 673$ K, $P_{O_2} = 3$ kPa.

include primarily oxidation reactions (CO, H_2, NH_3, CH_3OH, C_2H_4, C_2H_6, or C_3H_6 oxidation) and other types of reactions, including decomposition of CH_3NH_2, hydrogenation of C_2H_4, and reaction of NH_3 with NO [22]. Oscillatory behavior during the catalytic oxidation of propane was not reported until 2001, when oscillations were observed on Ni [25] and, more recently, on Pt [15].

Gladky et al. [25] observed oscillations during the catalytic oxidation of propane over a nickel wire. The reaction was studied at 873–1123 K, and the reacting mixture consisted of 95% propane and 5% oxygen. Oscillations were observed between 923 and 1023 K. The period of the oscillations was about 100 s, and the periodic changes in the reaction rate were accompanied by significant synchronous fluctuations of the catalyst temperature. At those temperatures, the reaction conversion was considerable in the absence of the Ni catalyst, and this observation originally led the authors to an interpretation of the oscillations through a mechanism involving both homogeneous and heterogeneous reaction steps. This same research group recently reported more detailed results [26,27]. By direct detection of free radicals, they found that the role of homogeneous reactions could not be significant in the mechanism of the observed oscillations. Also, XPS analysis showed that a thin (<100 nm) layer of NiO was formed on the catalyst surface during reaction. These results suggested periodic oxidation and reduction of the catalyst as the cause of the oscillatory phenomena. The high-reaction rate phase was associated with metallic nickel, whereas the low-activity phase was characterized by the presence of surface nickel oxide [26].

It is quite risky to consider the oscillatory phenomena observed in the present work necessarily of the same nature and origin as those reported by Gladky et al., not only because the catalyst was different, but also for the following reasons:

(a) The experimental conditions were quite different. In the case of Ni, the temperature range was 923–1023 K, and most of the oscillations were observed at low $P_{O_2}/P_{C_3H_8}$ ratios (typical inlet $P_{O_2}/P_{C_3H_8} = 0.053$). On Pt, the oscillatory data were obtained at $P_{O_2}/P_{C_3H_8}$ ratios of 1.2–2.2. Also, at temperatures above 723 K, only stable steady states were observed on Pt.

(b) In the present work, the conversions of either propane or oxygen were low (<10%). The catalyst temperature remained constant during the oscillations. Given the accuracy of the measurement, it is certain that the temperature could not fluctuate by more than 2–3 K. If the observed changes in the reaction rate were due to changes of the catalyst temperature only, then this fluctuation should be about 15–20 K. On Ni, on the other hand, temperature fluctuations as high as 100 K were observed.

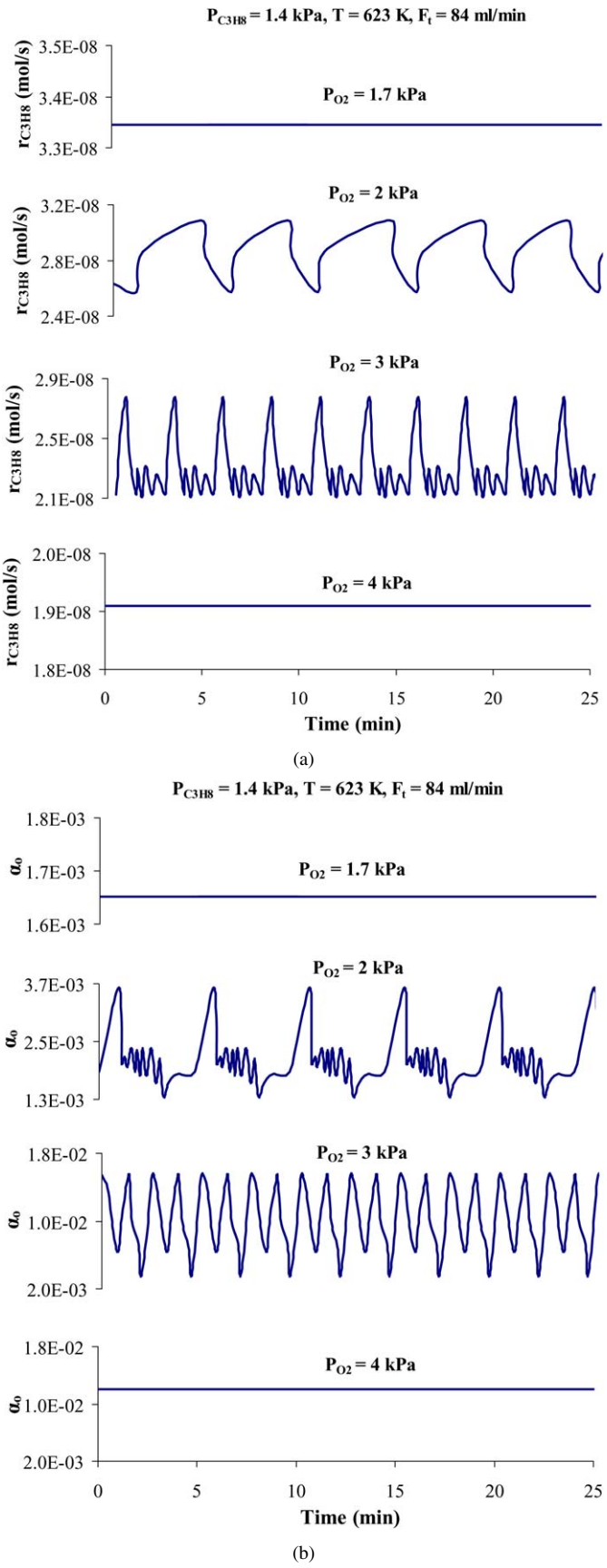

Fig. 5. Effect of P_{O_2} on (a) $r_{C_3H_8}$ and (b) α_o, at constant temperature. $T = 623$ K, $P_{C_3H_8} = 1.4$ kPa.

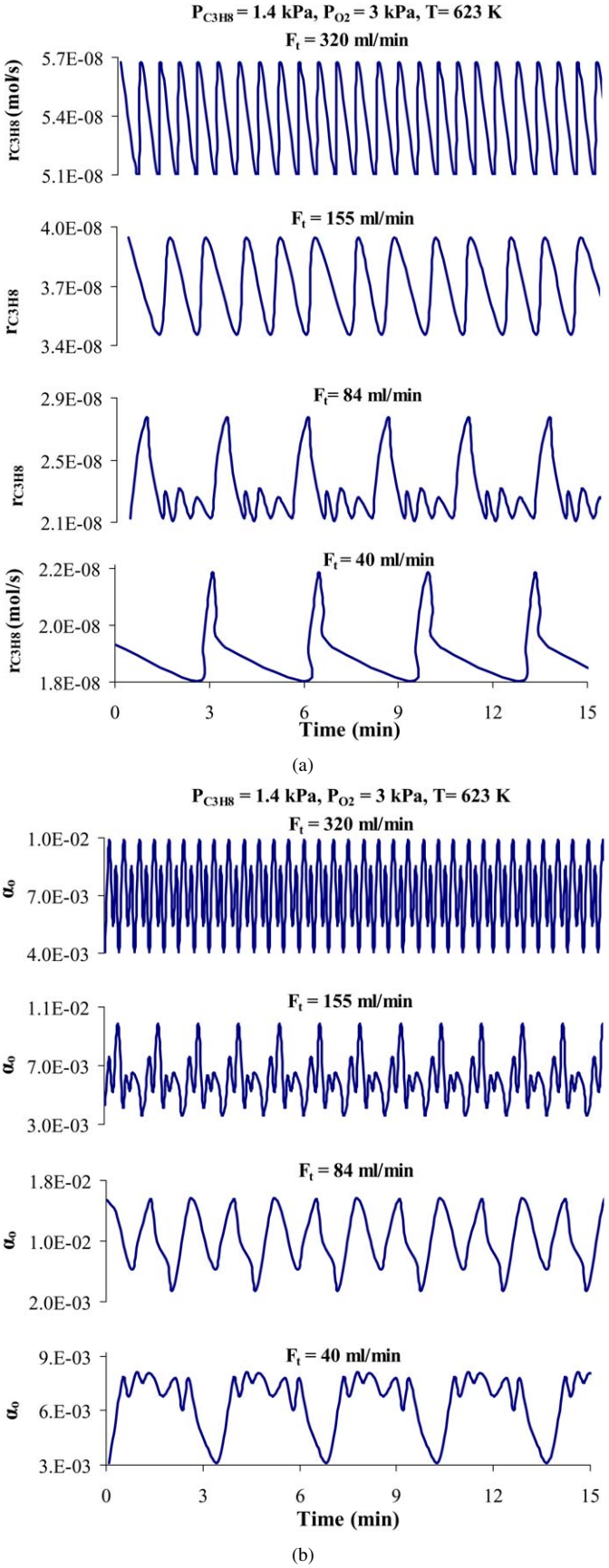

Fig. 6. Effect of residence time on (a) $r_{C_3H_8}$ and (b) α_o, at constant temperature and gas composition. $T = 623$ K, $P_{C_3H_8} = 1.4$ kPa, $P_{O_2} = 3$ kPa.

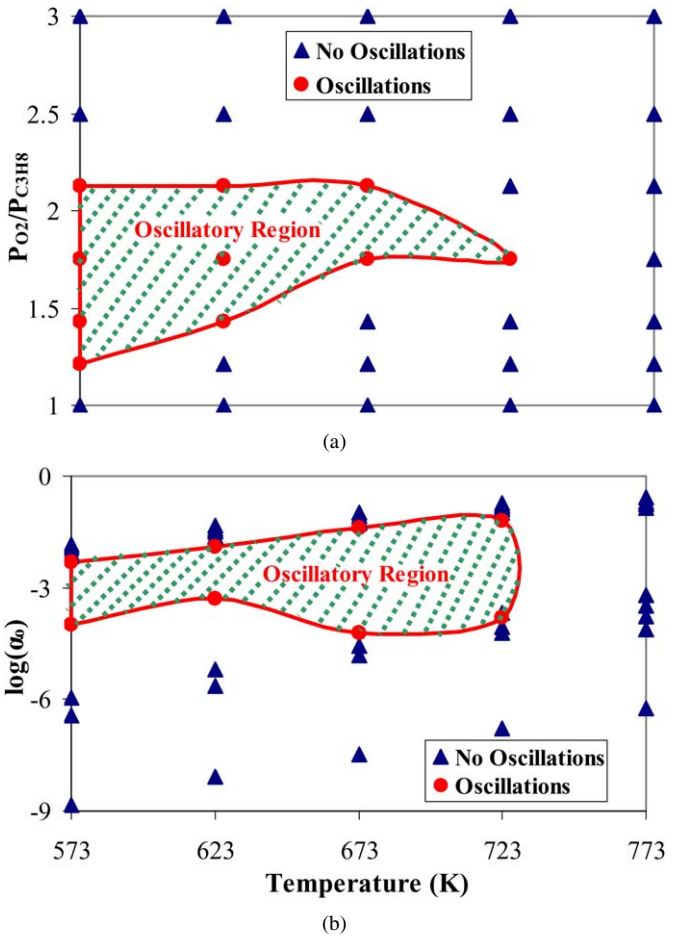

Fig. 7. Temperature effect on the upper and lower limits of (a) $P_{O_2}/P_{C_3H_8}$ and (b) $\log(\alpha_o)$, within which oscillations occur.

(c) On Ni, products of partial oxidation, such as CO and H_2, were detected in the effluent stream, but none of these products was detected in the present study. Oscillations have been observed in the catalytic oxidation of C_3H_6, CO, and H_2 on Pt [22–24]. If any of these compounds were among the products, then the observed oscillatory phenomena could be assumed related to the oxidation of that compound rather than to the oxidation of propane.

It is understood that any mechanism or model proposed for the interpretation of the oscillatory phenomena observed during the oxidation of propane on Pt should be in agreement with both the $r_{C_3H_8}$ and the α_o data. Thus, the SEP technique is helpful not only in obtaining in situ and continuous information about one of the reacting species (adsorbed oxygen), but also in excluding alternative models that fail to predict the α_o trends. So far, SEP has been used in studying other catalytic systems that exhibited sustained rate and α_o oscillations, including CO oxidation on Pt [34], C_2H_4 oxidation on Pt [35–37], H_2 oxidation on Ni [38–40], and propylene oxide oxidation on Ag [41,42]. SEP has also been used to study phase stability and phase changes, such as the decomposition of a metal oxide [43,44].

Detailed stable steady-state kinetic and SEP results of the catalytic oxidation of propane on Pt have been reported previously [15]. These results are summarized in Figs. 1 and 2. Figs. 1a and 1b show that a change in the dependence of the reaction rate with $P_{C_3H_8}$ is accompanied by an analogous change in the dependence of α_o. Fig. 1a shows that the reaction rate increases slowly with propane up to a certain $P_{C_3H_8}$, above which a sharper rate increase is observed. Because of the much smaller rate values, this change in the slope of rate versus $P_{C_3H_8}$ is not obvious at 573 and 623 K. The corresponding α_o values shown in Fig. 1b vary from 10^{-1} to 10^{-5} and decrease with increasing propane. It was shown previously [15] that if thermodynamic equilibrium were established between adsorbed and gaseous oxygen, then the α_o data should attain values on the order of 10^{-1} or higher. At temperatures in which a change in the slope of the reaction rate versus $P_{C_3H_8}$ occurs (e.g., 673–773 K), similar changes in the α_o versus $P_{C_3H_8}$ curves are observed. At 573 and 623 K, where there seems to be no change in the slope of the reaction rate curve, no sharp decrease in the α_o is observed either. Also, Fig. 1b shows that the oscillatory phenomena appear (shaded area) at $P_{C_3H_8}$ values within which the change from very high to very low α_o is observed.

Fig. 2a shows that at low P_{O_2}, the reaction rate is positive order in oxygen. After reaching a maximum, however, the reaction exhibits negative-order kinetics. Fig. 2b shows that at P_{O_2} where the reaction rate maxima are observed, very low oxygen activities are attained. As in Fig. 1b, at low P_{O_2}, where the reaction rate is higher, the deviation from equilibrium between adsorbed and gaseous oxygen is much stronger. Again, the oscillatory region appears at P_{O_2} values within which the α_o data shift drastically from very low to very high values (Fig. 2b). Also, in Fig. 2a, the shaded area (oscillatory region) is located at P_{O_2} values within which the reaction rate changes from positive to negative order with respect to oxygen.

An interpretation of the kinetic and potentiometric results of Figs. 1 and 2 has been proposed previously [15]. The two regions of Fig. 1 (high and low $P_{O_2}/P_{C_3H_8}$) are associated with the oxidation of the catalyst and formation of surface oxide, on which the reaction rate is significantly lower than on the reduced catalyst. At high $P_{O_2}/P_{C_3H_8}$, the Pt surface is oxidized, and low reaction rates are attained. At low $P_{O_2}/P_{C_3H_8}$, the surface is reduced, and thus it becomes much more active for propane oxidation. A high reaction rate means that the steady-state value of α_o will be very low. The picture is quite similar in Fig. 2, which plots $r_{C_3H_8}$ and α_o versus P_{O_2}. At low P_{O_2}, the catalyst is reduced, and high reaction rates are observed. As P_{O_2} increases, the Pt surface is gradually oxidized, and its catalytic activity drops. Hence, after reaching a maximum, the rate decreases with P_{O_2}.

In addition to the stable steady-state behavior, it is also possible to obtain a qualitative interpretation of the observed oscillations assuming periodic oxidation and reduction of the catalyst surface. Gaseous oxygen adsorbs dissociatively on Pt. The catalyst surface can also undergo oxidation to form PtO_2. However, the reaction of PtO_2 formation can occur only if the surface oxygen activity exceeds a minimum value of α_o^*.

This periodic oxidation and reduction of the catalyst surface provides a physical interpretation of the appearance and disappearance of the oscillatory phenomena. Fig. 8 shows schemati-

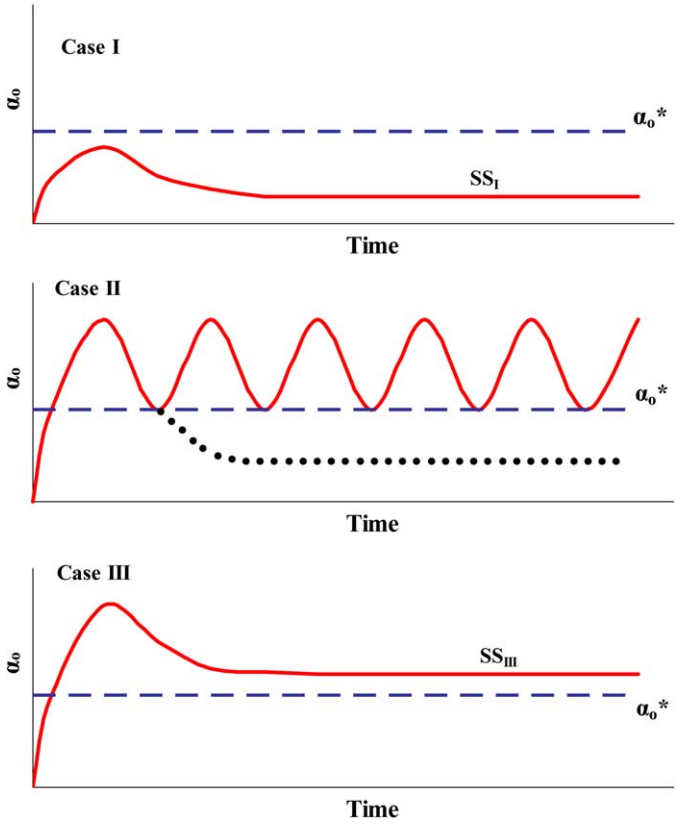

Fig. 8. Transient behavior of surface oxygen activity. Cases I and III: Stable steady states only. Case II: Oscillatory behavior.

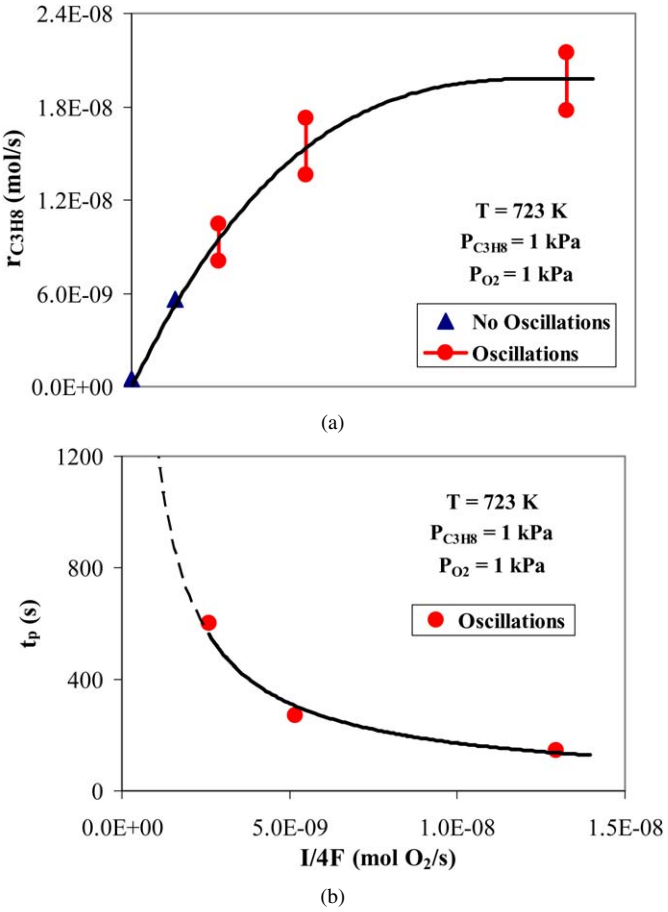

Fig. 9. Dependence of (a) the reaction rate, $r_{C_3H_8}$, and (b) the period of oscillations, t_p, on the imposed current. $T = 723$ K, $P_{O_2} = 1$ kPa, $P_{C_3H_8} = 1$ kPa.

cally the existence of oscillatory and stable steady-state regions depending on α_o^*, the critical value for PtO_2 formation. At $t = 0$, the catalyst surface is assumed to be in its metallic state. Reactant gases are fed into the reactor, gaseous oxygen adsorbs, and the surface oxygen activity, α_o, increases. For very low inlet P_{O_2}, the surface oxygen activity attains values below the minimum α_o^* required to form the oxide. Hence, stable steady states are observed (SS_I), and the catalyst is in its reduced form. This situation corresponds to case I in Fig. 8 and also to the areas below the oscillatory regions in Figs. 7a and 7b. Case II corresponds to intermediate values of inlet P_{O_2}. In this case, α_o increases sharply and exceeds the value of α_o^*. Therefore, formation of PtO_2 is possible. Because of the oxide formation, however, the number of metallic sites available for oxygen adsorption starts to decrease. Consequently, after going through a maximum, α_o starts to decrease to reach a steady-state value (horizontal black circles in case II of Fig. 8). Before reaching that steady state, however, α_o hits the stability limit α_o^*. This means that the oxide is now unstable, and it decomposes to create "clean" Pt sites. When the oxide becomes unstable, it reacts rapidly with propane and increases the oxygen/propane ratio, thus starting the next cycle. This mechanism can also explain the effect of gas flow rate on the period of oscillations; at high flow rates (i.e., short residence times), changes in the oxygen/propane ratio occur faster, thus reducing the period of the cycle (Fig. 6). Case III corresponds to very high values of inlet P_{O_2}. For very high P_{O_2}, the steady-state value of α_o that the system tends to reach (SS_{III}) exceeds the stability limit α_o^*; therefore, the oxide that has been formed is stable and does not decompose. Limit cycles do not appear, and the surface is primarily oxidized. Case III in Fig. 8 corresponds to the areas above the oscillatory regions in Figs. 7a and 7b.

The proposed interpretation is also supported by the closed-circuit results reported previously, where the effect of electrochemical promotion (NEMCA) on propane oxidation was investigated [15]. An example of these closed-circuit experiments is shown in Fig. 9. The inlet composition and the reactor temperature were kept constant ($P_{C_3H_8} = P_{O_2} = 1.0$ kPa, $T = 723$ K). Under open circuit (i.e., with no current passing through the solid electrolyte), and with both reactants co-fed as gaseous C_3H_8 and O_2, the cell reactor operated as a regular catalytic reactor. Under closed circuit, the cell reactor operated as an electrochemical oxygen "pump"; a current (I) was imposed through the oxygen ion (O^{2-}) conducting solid electrolyte. This current corresponds to a flux of $I/4F$ mol of oxygen/s. Fig. 9a shows that under an open circuit ($I = 0$), a stable steady-state rate of 5.2×10^{-10} mol/s was obtained. On imposing a current of $I = 0.5$ mA, the rate increased to a new stable steady-state value of 5.6×10^{-9} mol/s. But when the current was increased to 1.0 mA, the reaction rate started to oscillate. The period was about 560 s at $I = 1$ mA and decreased to about 260 s at $I = 2$ mA and to 150 s at $I = 5$ mA (Fig. 9b).

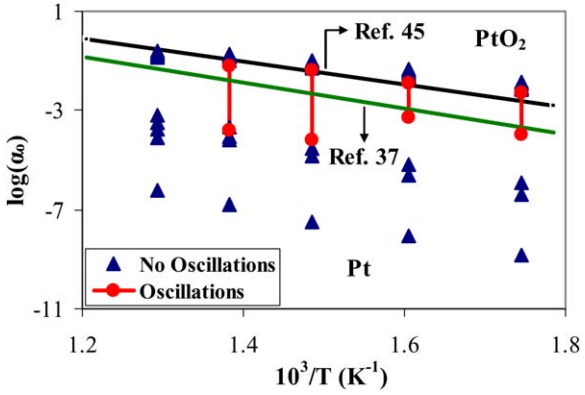

Fig. 10. Oscillatory and stable steady-state values of α_o compared to literature values for the stability limit of PtO_2.

Apparently, the data of Fig. 9 are in disagreement with those of Fig. 7a, which show that the reaction does not oscillate at $T = 723$ K and $P_{O_2}/P_{C_3H_8} = 1.0$. By imposing a current, however, additional oxygen is "pumped" directly to the Pt surface. A flux of oxygen is electrochemically brought to the catalyst surface through the solid electrolyte (as O^{2-}) and should be added to oxygen brought to the surface via adsorption from gaseous O_2. A simple algebraic addition of gaseous and electrochemical oxygen does not bring the $P_{O_2}/P_{C_3H_8}$ into the oscillatory region. It is understood, however, that the nature of the electrochemically supplied O^{2-} is quite different from that of gaseous O_2. This is also shown by the strongly nonfaradaic electrochemical promotion effect on the reaction rate; the increase in the rate of oxygen consumption was found to exceed the rate of O^{2-} supply to the catalyst by up to 1200 times [15].

The equilibrium constant K for the reaction of PtO_2 formation determines a temperature-dependent critical surface oxygen activity α_o^* below which the oxide becomes unstable, that is,

$$K = 1/(\alpha_o^*)^2 \tag{2}$$

or, equivalently,

$$\alpha_o^* = 1/K^{0.5}. \tag{3}$$

Fig. 10 contains the experimentally observed dependence on temperature of the α_o values within which the reaction exhibits either stable steady states (triangles) or oscillatory behavior (circles connected with a straight line). Also shown on the same figure are literature values [37,45] for the dissociation of PtO_2. Reference [45] is the work of R.J. Berry, who used an electrical resistance technique to measure the formation of the oxide on polycrystalline platinum wires. Reference [37] is the work of Michaels and Vayenas, who used SEP to study rate and oxygen activity oscillations observed during the oxidation of C_2H_4 on Pt. It can be seen that the lines from Refs. [37] and [45] fall very close to the α_o^* values determined experimentally in the present work. Hence, although not proved conclusively, the proposed interpretation of the oscillatory phenomena as being related to the periodic formation and decomposition of platinum oxide is in good agreement with previous findings reported in the literature.

5. Conclusion

The reaction rate and surface oxygen activity oscillations observed during the catalytic oxidation of propane on Pt are affected by the gas-phase composition, catalyst temperature, volumetric flow rate, and electrochemical supply of oxygen through the solid electrolyte. At each temperature, there was a minimum and a maximum $P_{O_2}/P_{C_3H_8}$ ratio within which the reaction exhibited oscillations. Oscillatory phenomena were not observed at temperatures above 723 K regardless of the reactant composition. The reaction rate and primarily the SEP data strongly indicate that the oscillatory phenomena are related to formation and decomposition of a surface platinum oxide.

Acknowledgments

The authors acknowledge financial support for this research from the General Secretariat of Research and Technology of Greece under the PENED 2003 Programme.

References

[1] A.F. Lee, K. Wilson, R.M. Lambert, C.P. Hubbard, R.G. Hurley, R.W. McCabe, H.S. Gandhi, J. Catal. 184 (1999) 491.
[2] C.P. Hubbard, K. Otto, H.S. Gandhi, K.Y.S. Ng, J. Catal. 139 (1993) 268.
[3] L. Kiwi-Minsker, I. Yuranov, E. Slavinskaia, V. Zaikovskii, A. Renken, Catal. Today 59 (2000) 61.
[4] Y. Yazawa, N. Takagi, H. Yoshida, S. Komai, A. Satsuma, T. Tanaka, S. Yoshida, T. Hattori, Appl. Catal. A: Gen. 233 (2002) 103.
[5] T.F. Garetto, E. Rincón, C.R. Apesteguía, Appl. Catal. B: Environ. 48 (2004) 167.
[6] H. Yoshida, Y. Yazawa, T. Hattori, Catal. Today 87 (2003) 19.
[7] A. Ishikawa, S. Komai, A. Satsuma, T. Hattori, Y. Murakami, Appl. Catal. A: Gen. 110 (1994) 61.
[8] Y. Yazawa, H. Yoshida, T. Hattori, Appl. Catal. A: Gen. 237 (2002) 139.
[9] R. Burch, E. Halpin, M. Hayes, K. Ruth, J.A. Sullivan, Appl. Catal. B: Environ. 19 (1998) 199.
[10] C.P. Hubbard, K. Otto, H.S. Gandhi, K.Y.S. Ng, J. Catal. 144 (1993) 484.
[11] H. Wu, L. Liu, S. Yang, Appl. Catal. A: Gen. 211 (2001) 159.
[12] A. Hinz, M. Skoglundh, E. Fridell, A. Anderson, J. Catal. 201 (2001) 247.
[13] P. Vernoux, F. Gaillard, L. Bultel, E. Siebert, M. Primet, J. Catal. 208 (2002) 412.
[14] N. Kotsionopoulos, S. Bebelis, J. Appl. Electrochem. 35 (2005) 1253.
[15] C. Kokkofitis, G. Karagiannakis, S. Zisekas, M. Stoukides, J. Catal. 234 (2005) 476.
[16] P. Hugo, in: 4th European Symposium on Chemical Reaction Engineering, Brussels, 1968, Pergamon, Oxford, 1971, p. 459.
[17] P. Hugo, Ber. Bunsen. Phys. Chem. 74 (1970) 121.
[18] E. Wicke, H. Beusch, P. Fieguth, ACS Symp. Ser. 109 (1972) 615.
[19] M. Sheintuch, R.A. Schmitz, Catal. Rev.—Sci. Eng. 15 (1977) 107.
[20] M.G. Slin'ko, M.M. Slin'ko, Catal. Rev.—Sci. Eng. 17 (1978) 119.
[21] L.F. Razon, R.A. Schmitz, Catal. Rev.—Sci. Eng. 28 (1986) 89.
[22] F. Shuth, B.E. Henry, L.D. Schmidt, Adv. Catal. 39 (1993) 51.
[23] M.M. Slin'ko, N.I. Jaeger, in: B. Delmon, J.T. Yates (Eds.), Studies in Surface Science and Catalysis, vol. 86, Elsevier, Amsterdam, 1994.
[24] R. Imbihl, G. Ertl, Chem. Rev. 95 (1995) 697.
[25] A.Yu. Gladky, V.K. Ermolaev, V.N. Parmon, Catal. Lett. 77 (2001) 103.
[26] A.Yu. Gladky, V.V. Kaichev, V.K. Ermolaev, V.I. Bukhtiyarov, V.N. Parmon, Kinet. Catal. 46 (2005) 251.
[27] A.Yu. Gladky, V.V. Ustagov, A.M. Sorokin, A.I. Nizovskii, V.N. Parmon, V.I. Bukhtiyarov, Chem. Eng. J. 107 (2005) 33.
[28] C.G. Vayenas, S.I. Bebelis, I.V. Yentekakis, H.-G. Lintz, Catal. Today 11 (1992) 303.

[29] I. Metcalfe, Catal. Today 20 (1994) 283.
[30] C.G. Vayenas, M.M. Jaksic, S. Bebelis, S.G. Neophytides, in: J.O'.M. Bockris, B.E. Conway, W.R.E. White (Eds.), Modern Aspects in Electrochemistry, vol. 29, Plenum, New York, 1996, p. 57.
[31] C.G. Vayenas, S. Bebelis, C. Pliangos, S. Brosda, D. Tsiplakides, Electrochemical Activation of Catalysis, Kluwer Academic/Plenum, New York, 2001.
[32] M. Estenfelder, T. Hahn, H.-G. Lintz, Catal. Rev.—Sci. Eng. 46 (2004) 1.
[33] M. Stoukides, Catal. Rev.—Sci. Eng. 42 (2000) 1.
[34] I.V. Yentekakis, S. Neophytides, C.G. Vayenas, J. Catal. 111 (1988) 152.
[35] C.G. Vayenas, B. Lee, J.N. Michaels, J. Catal. 66 (1980) 36.
[36] C.G. Vayenas, C. Georgakis, J.N. Michaels, J. Tormo, J. Catal. 67 (1981) 348.
[37] C.G. Vayenas, J.N. Michaels, Surface Sci. 120 (1982) L405.
[38] C. Saranteas, M. Stoukides, J. Catal. 93 (1985) 417.
[39] D. Eng, M. Stoukides, T. McNally, J. Catal. 106 (1987) 342.
[40] H. Arif, M. Stoukides, Chem. Eng. Sci. 41 (1986) 945.
[41] M. Stoukides, C.G. Vayenas, J. Catal. 74 (1982) 266.
[42] M. Stoukides, S. Seimanides, C.G. Vayenas, ACS Symp. Ser. 196 (1982) 165.
[43] E. Häfele, H.-G. Lintz, Solid State Ionics 23 (1987) 235.
[44] H.H. Hildenbrand, H.-G. Lintz, Catal. Today 9 (1991) 153.
[45] R.J. Berry, Surface Sci. 76 (1978) 415.